Journal of Robotics and Control (JRC)
Volume 6, Issue 3, 2025
ISSN: 2715-5072, DOI: 10.18196/jrc.v6i3.26440

Design and Simulation of a Multi-Stage On-Site System for Hazardous Medical Waste Treatment in Low-Resource Healthcare Settings

Roger Fernando Asto Bonifacio [1*], Blanca Yeraldine Buendia Milla [2], Jezzy James Huaman Rojas [3]
[1, 2, 3] Department of Mechatronic Engineering, Faculty Engineering, Universidad Continental, Huancayo, Perú
Email: [1] 71866336@continental.edu.pe, [2] 73272335@continental.edu.pe, [3] jhuamanroj@continental.edu.pe
*Corresponding Author

***Abstract*—The management of hazardous medical waste in rural settings with limited resources faces significant constraints due to the lack of specialized infrastructure and inefficiencies in collection systems. This study presents the design and theoretical validation of a compact multi-stage system that integrates five key processes: double shredding, thermal evaporation, gas purification, hydraulic compaction, and UV-C disinfection. The methodology involved finite element analysis (FEA) to verify the shredding subsystem's structural integrity and thermal simulations to assess the efficiency of the evaporation process and the thermal safety of the equipment. Results obtained using SimSolid showed safety factors greater than 2.5 in critical shaft and blade regions, with structural displacements below 0.21 mm. Thermal simulations indicated that the chamber reached operating temperatures between 400 and 600 °C within 20 to 25 minutes, while the external surface remained below 60 °C due to the use of refractory insulation. A consistent thermal response was observed even under extreme simulated conditions (700-1100 °C), reinforcing the design's stability. The combined heat treatment and compaction stages enabled an estimated waste volume reduction of 70% to 75%. In addition, the microbiological neutralization potential of the system, based on advanced filtration and UV-C disinfection, was evaluated, acknowledging simulation limitations and the need for future experimental validation. The primary contribution of this work lies in demonstrating the feasibility of an autonomous, safe, and efficient system for on-site hazardous medical waste treatment. Future work will focus on building a functional prototype, conducting real-world testing, and analyzing energy consumption and adaptability in rural settings with variable infrastructure.**

***Keywords*—Medical Waste; On-Site Treatment; Mechatronic Design; FEA Simulation; Thermal Evaporation; UV-C Disinfection.**

I. INTRODUCTION

The safe management of medical waste remains a persistent challenge for healthcare systems, both in developed infrastructures and in resource-limited settings. Several studies have shown that the generation of hospital waste is closely related to population density and local treatment capacity, which increases the risk of exposure to infectious agents, especially during health emergencies [1]-[3].

This issue is further exacerbated in rural regions due to the sustained expansion of medical services and the intensive use of disposable supplies, resulting in a higher burden of hazardous waste. In these areas, limited energy availability requires solutions that are compatible with renewable sources or have low energy consumption [4]. Although various strategies have been developed, ranging from optimizing collection routes and waste-to-energy conversion to chemical and thermal treatment technologies [5]-[8], most of these solutions are tailored for urban environments and are not feasible in rural communities due to their reliance on specialized infrastructure and trained personnel.

In the Peruvian context, this gap is particularly evident in rural health posts, where the prolonged accumulation of items such as syringes, gloves, masks, and plastic bottles poses a concrete risk to public health [9]-[11]. While decentralized energy solutions, such as mobile stations or photovoltaic systems implemented during the pandemic, have been applied in these settings [12], there is still a lack of compact technologies that enable the on-site pretreatment of hazardous medical waste. Current technologies tend to fragment treatment stages or require technical conditions that are difficult to replicate in remote areas [13]-[16].

To address this gap, this study proposes the design and simulation of a compact machine that integrates, within a single automated system, the processes of double shredding, thermal evaporation, gas emission purification, and UV-C disinfection, aiming to reduce both the volume and microbiological load of waste generated in rural healthcare facilities. The innovation lies in combining these treatment stages through a low-power mechatronic control system that is adaptable to isolated operational conditions.

The main contribution of this research is the development of a comprehensive solution adapted to the technical, energy, and environmental constraints of the Peruvian rural environment. To this end, finite element simulations (FEA) and thermal analyses were conducted to validate the structural and functional feasibility of the proposed design, laying the groundwork for the construction of a physical prototype to be experimentally evaluated in real-world scenarios.

II. COMPACT MACHINE ARCHITECTURE

The compact machine's design is based on the functional integration of five main subsystems: double shredding, thermal evaporation, gas emission purification, hydraulic compaction, and UV-C radiation disinfection. This architecture is managed by an automated mechatronic system

capable of operating in rural environments with limited technical personnel. The system enables safe, autonomous, and efficient handling of hazardous medical waste by regulating critical variables such as shredding speed, evaporation temperature, and cleaning cycles [17], [18].

A. Shredding Subsystem

The shredding subsystem reduces the size of medical waste before thermal treatment [19], [20]. It comprises:

- Primary Shredder A: Designed to process high-hardness waste (syringes, bottles, gloves).
- Secondary Shredder B: Reduces the material from the primary stage to a 1-5 mm particle size, enhancing thermal efficiency.

Both units are represented in the conceptual diagram shown in Fig. 1, which shows the rotary blades, shafts, supports, and transmission mechanism.

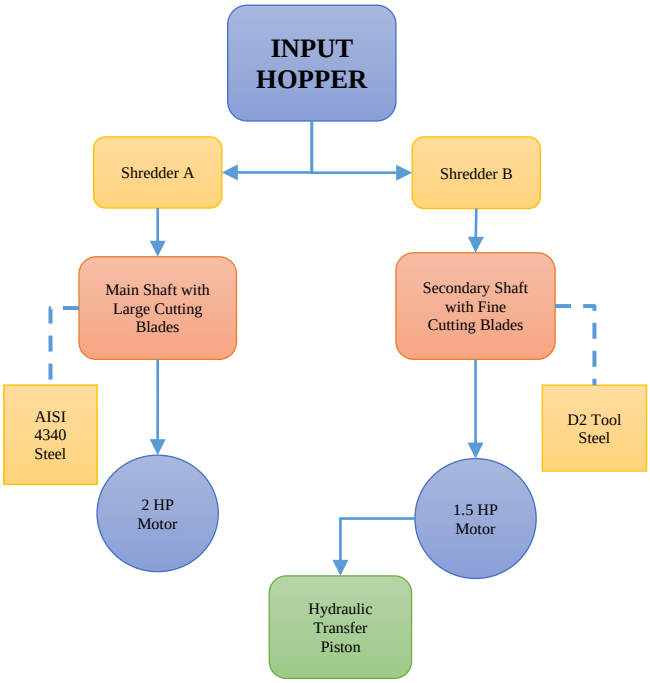

Fig. 1. Conceptual diagram of the shredding subsystem

Shredder A uses AISI 4340 hardened steel blades (55-60 HRC), known for their high toughness and impact resistance [21]. Shredder B features D2 steel blades (58-62 HRC), which maintain sharpness under prolonged use [22]-[27]. The shredders are powered by 2 HP and 1.5 HP motors, respectively, controlled by variable frequency drives that allow operation between 100 and 200 rpm, depending on the waste type and processing stage.

B. Thermal Evaporation Chamber

This module replaces traditional incineration with the controlled application of heat to degrade waste without direct combustion. Fig. 2 shows its cylindrical structure, equipped with thermal insulation and distributed electric resistors [28], [29].

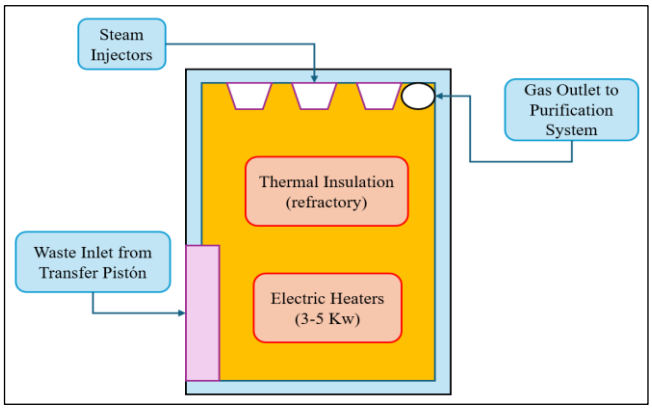

Fig. 2. Evaporation process diagram

It operates between 400 and 600 °C, using 3-5 kW resistors regulated by type-K thermocouples and a PID control system. A hydraulic piston transfers shredded waste into the chamber, while refractory insulation minimizes thermal losses, ensuring operator safety. This stage allows a 40% to 50% reduction in the initial volume, preventing the excessive formation of toxic compounds such as dioxins [30].

C. Gaseous Emissions Purification System

After evaporation, the generated vapors and gases are directed to an advanced purification system composed of:

- Baking soda ($NaHCO_3$) injection: Neutralizes acidic compounds such as chlorides and oxides.
- Activated carbon filter: Captures volatile organic compounds (VOCs), trace amounts of heavy metals, and odors.
- Mechanical filter: Retains solid particles.
- Controlled ventilation system.

With this, emissions meet safety standards and minimize environmental impact [31], [32].

D. Final Post-Processing and Control Subsystems

After thermal evaporation, the system executes an automated sequence of complementary processes, illustrated in Fig. 3, to achieve microbiological neutralization, final volume reduction, and hygienic maintenance.

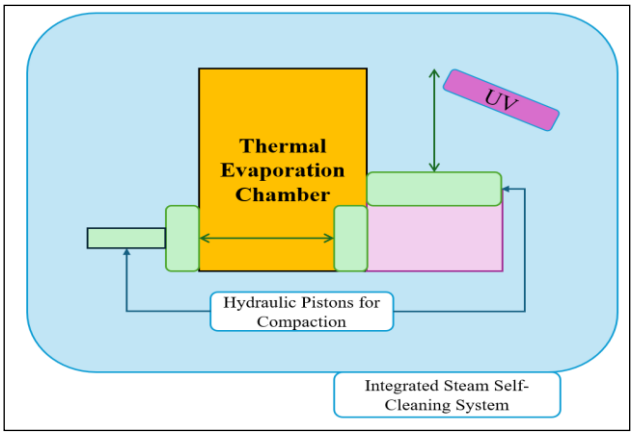

Fig. 3. Diagram of final processes for the management of medical waste

First, the treated solid waste is compacted by lateral hydraulic pistons to form dense and stable blocks. This facilitates safe handling, storage, and transportation while minimizing residual particle dispersion. Next, the waste passes through a sealed UV-C disinfection chamber equipped with 254 nm lamps. This stage adds a biosafety barrier by inactivating remaining microorganisms. Safety interlocks prevent access while the lamps are active. Studies indicate that doses above 100 J/m² are effective for sterilization [33]-[36].

To maintain system hygiene and prevent contamination buildup, a steam self-cleaning subsystem periodically sanitizes the feed hopper, shredders, and internal ducts. The steam is generated using a heat exchanger that recycles waste heat and is distributed through strategically positioned spray nozzles [37]-[41]. All processes are coordinated by a mechatronic control system that integrates distributed sensors and actuators. The system includes variable frequency drives, PID controllers, automatic UV activation, compaction, and cleaning routines. Temperature, pressure, and current sensors enable continuous monitoring of the operational status and trigger safety alarms in the event of faults [42]-[48].

III. SIMULATION METHODOLOGY

This section presents the computational simulation strategy implemented for the preliminary validation of a multistage system intended for the on-site treatment of hazardous medical waste in rural, low-resource environments [49], [50]. The proposed system integrates four sequential subsystems: primary and secondary shredding, thermal evaporation, gas purification, and UV-C radiation disinfection into a compact, autonomous unit. The main objective of the simulation was to verify the structural and thermal feasibility of the design prior to prototype fabrication and field deployment.

The methodological procedure was divided into two main simulation lines:

1) Mechanical stress analysis (FEA): The structural strength of the critical components of the shredding subsystem, including blades, shafts, and structural supports, subjected to dynamic loads, was evaluated. A fatigue analysis under cyclic loading was also configured.

2) Heat transfer simulation: The heat transfer behavior in the evaporation chamber, including conduction, convection, radiation, and forced ventilation dissipation, was modeled. The gas purification stage was considered at a functional level but was not included in the computational simulation [51]-[54].

3) Sensitivity analysis: A qualitative sensitivity study was conducted to identify the system design's robustness to variations in key parameters. These included material properties, thermal insulation performance, energy supply variability, and waste volume per treatment cycle [55], [56].

Fig. 4 summarizes the simulation workflow from CAD modeling to analysis and interpretation. It outlines the interconnection between mechanical and thermal evaluations and highlights their contribution to the overall system validation process.

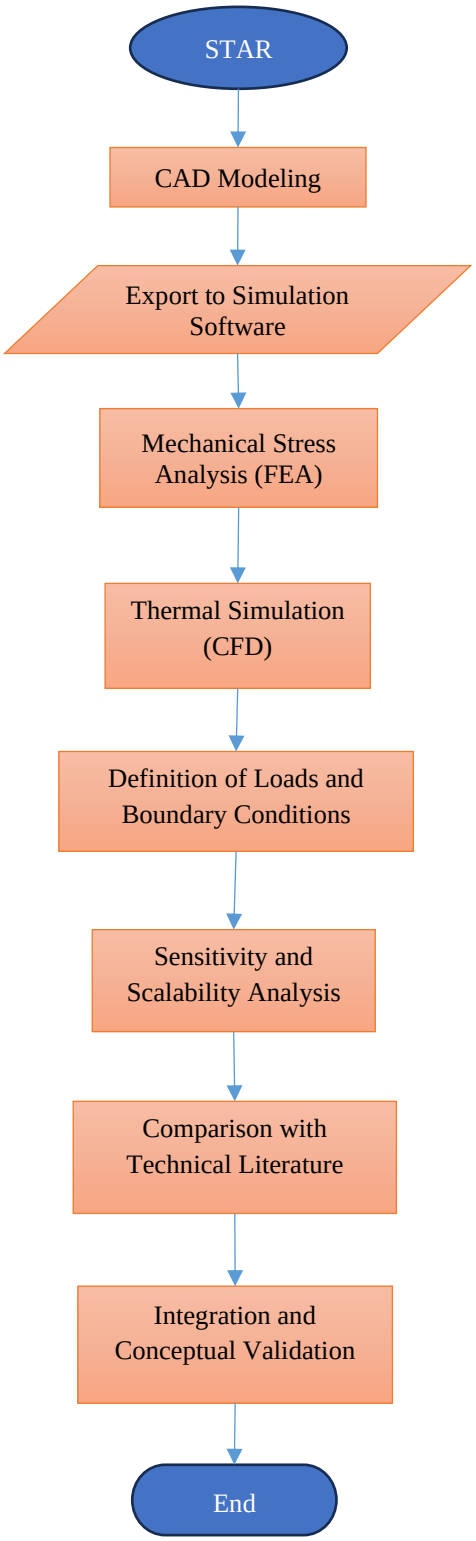

Fig. 4. Flowchart of the simulation and conceptual validation process

A. Mechanical Stress Analysis (FEA)

The objective of the mechanical stress analysis was to verify whether the shredding subsystem's rotating blades and drive shafts operated within the allowable limits for the selected materials. Three types of steel were used: AISI 4340 for the primary shredder, D2 for the secondary shredder, and ASTM A36 for the shafts and structural supports [57], [58]. The relevant mechanical properties are shown in Table I.

TABLE I. MECHANICAL PROPERTIES OF THE MATERIALS USED

Components	Parameters		
	Material	***Elastic limit (MPa)***	***Tensile strength (MPa)***
Shredder A	AISI 4340 Steel	745	1080
Shredder B	D2 Steel	735	980
Brackets & shafts	ASTM A36 Steel	250	400

The geometric model was developed using CAD software and included the shredding units, drive shafts, hydraulic pistons, and supporting structures [59]-[62]. Fig. 5 presents the 3D assembly of the subsystem. The model was exported to the SIMSOLID simulation environment, where the finite element analyses were performed. A mesh refinement was applied to critical zones, especially at the blade-shaft interface and the coupling points between the shredders and the structural chassis [63]-[65].

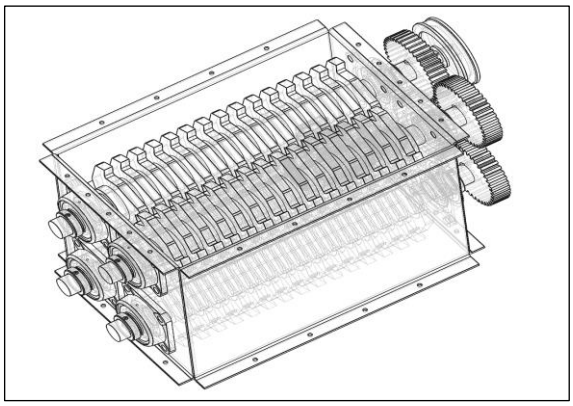

Fig. 5. CAD model of the shredding and compaction system

The loading conditions included the maximum torque applied to each shaft, calculated from the rated power of the electric motors (1.5-2 HP), and the impact forces generated during medical waste processing, estimated at a volume of 10-15 liters per cycle. The maximum pressure exerted by the hydraulic pistons during compaction was also considered. Boundary conditions were applied at the fixed supports located in the bearings, chassis, and guides of the compaction system [66], [67].

The structural evaluation was based on the Von Mises equivalent stress criterion and the calculation of the safety factor (FoS), with special attention given to high-stress regions such as the blade-shaft junctions [68]-[72]. Finally, a fatigue analysis under cyclic loading conditions representative of prolonged operation in rural zones was implemented to identify areas prone to stress concentrations and potential fatigue-induced cracks.

B. Heat Transfer Simulation

The objective of the heat transfer analysis was to evaluate the evaporation chamber's capacity to reach and maintain temperatures in the range of 400 to 600 °C, which are considered suitable for the thermal degradation and evaporation of hazardous medical waste [73]. Fig. 6 shows the three-dimensional model of the evaporation chamber developed for this purpose.

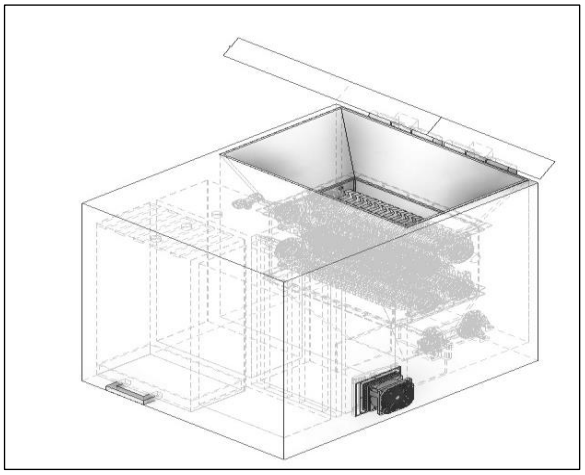

Fig. 6. Three-dimensional model of the compact machine in SolidWorks software

The thermal simulation included defining internal heat sources by modeling electrical resistors distributed uniformly throughout the chamber volume, with a total estimated power between 3 and 5 kW. A uniform heat distribution was assumed as the baseline hypothesis to evaluate heat transfer efficiency under ideal conditions [74], [75].

With respect to boundary conditions, controlled input flows were defined to represent the transfer of solid waste from the shredding system into the evaporation chamber. The cyclic motion of the transfer piston, responsible for intermittently introducing the shredded material, was also modeled [76], [77].

Although the system design includes a gas purification stage through the injection of neutralizing agents, such as sodium bicarbonate, this stage was only addressed functionally and was not included in the simulation phase of this study [78]-[82]. The analysis focused exclusively on heat transfer phenomena within the chamber, while gas flow dynamics and neutralization were deferred to future validation stages.

The model considered multiple heat transfer mechanisms: conduction through the refractory lining, internal convection generated by the movement of air and gases, thermal radiation between internal surfaces, and forced ventilation for gas extraction. Table II details the thermal properties of the materials used in the simulation.

TABLE II. THERMAL PROPERTIES OF THE MATERIALS USED IN THE SIMULATION

Material	Properties		
	Thermal Conductivity (W/m*K)	***Heat Capacity (J/kg*K)***	***Density (kg/m³)***
Refractory lining	1.2	800	2200
Structural Steel (casing)	45	500	7850
Air (internal flow)	0.026	1005	1.225

C. Sensitivity Analysis

To evaluate the proposed system's robustness under variable operating conditions, a sensitivity analysis focusing on the most critical design parameters was carried out. This methodological stage was particularly relevant given that the system is intended for rural environments, where fluctuations in energy supply, alternative construction materials, and variations in waste composition are expected [83]-[88].

The qualitative impact of individual variations was assessed for the following variables:

1) Mechanical properties of materials: A margin of ±15% was evaluated for the yield strength and tensile strength of the selected steels (AISI 4340, D2, and ASTM A36), considering potential substitutions with locally available materials.

2) Supplied thermal power: The chamber's heating elements were considered to have an operational range between 3 and 5 kW, reflecting scenarios of energy limitations or reduced efficiency.

3) Thermal conductivity of the insulation: Variations of ±20% in the conductivity of the refractory material were analyzed, anticipating the use of alternative compounds with differing thermal capacities.

4) Load volume per cycle: Operational scenarios between 10 and 20 liters per cycle were estimated, associated with different densities and types of medical waste.

This analysis helped identify the system components most sensitive to external variations and provided preliminary safe operating ranges. Although a formal probabilistic approach was not applied, the proposed scenarios offer a practical basis for future optimization and will guide subsequent phases of experimental validation under real-world conditions.

IV. RESULTS

A. Mechanical Stress Analysis (FEA)

The finite element analysis (FEA) was conducted to evaluate the structural integrity of the double-shredding subsystem, considering the load conditions and constraints described in Section III.A. The materials assigned were AISI 4340 alloy steel for the primary shredder, D2 tool steel for the secondary shredder, and ASTM A36 structural steel for the shafts and support components, following the values reported in Table I.

The 3D model was exported to the SIMSOLID environment, where equivalent torques generated by 1.5 to 2 HP electric motors were applied. To replicate realistic operational conditions, boundary conditions were imposed on the bearings and chassis.

The results revealed a homogeneous stress distribution across most critical regions. Fig. 7 presents the Von Mises stress map:

- (a) For the primary shredder, where stress concentrations are detected at the interface between the shaft and the blades,
- (b) For the secondary shredder, a lower load is observed, according to the lower torque applied.

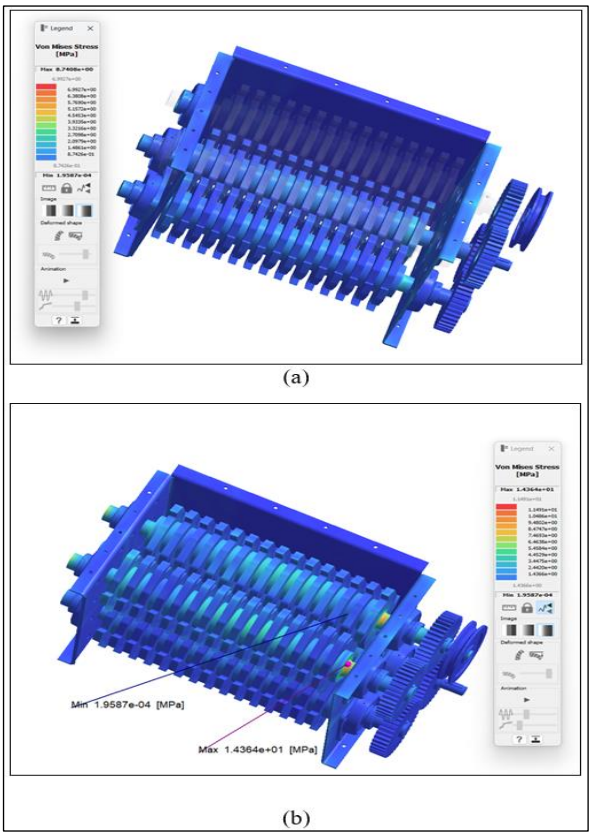

Fig. 7. Von Mises stress distribution in the shredding subsystem: (a) Primary shredder and (b) Secondary shredder

The maximum stress recorded was 14.36 MPa, representing only 1.8% of the yield strength of the materials used (above 800 MPa). This large margin indicates a high resistance to nominal mechanical loads.

Fig. 8 illustrates the displacement map under simulated loading. The maximum deformation was 0.21 mm, located at the periphery of the primary blade, without compromising alignment or functionality.

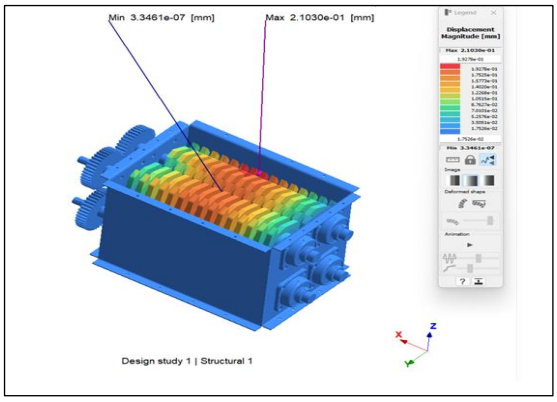

Fig. 8. Map of total displacements of the assembly under simulated load conditions

The safety factor (FoS) analysis, shown in Fig. 9, revealed a minimum value of 6.16, which significantly exceeds the design threshold of 2.5. This suggests the system would

maintain structural stability even under more severe conditions or with slightly lower mechanical properties.

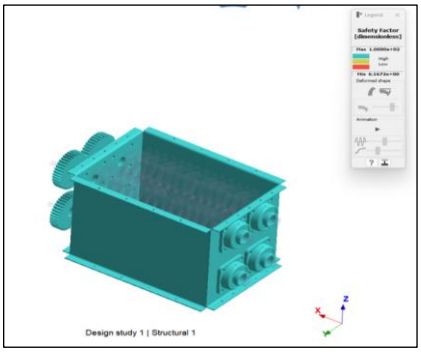

Fig. 9. Safety Factor (FoS) map obtained in the FEA analysis

Finally, a fatigue simulation under cyclic loading estimated a minimum service life of 5,000 cycles before the initiation of microcracks or significant structural wear. This estimate should be considered preliminary and subject to experimental validation in subsequent phases. Geometric imperfections and manufacturing tolerances were not included in this stage. Therefore, periodic inspection of welds and corrective maintenance of blades and shafts are recommended to ensure operational safety under prolonged use.

B. Thermal Analysis Results

Thermal simulations were performed to assess the evaporation chamber's ability to reach and maintain temperatures suitable for the degradation of hazardous medical waste, estimated between 400 and 600 °C [47]-[50]. Additionally, the effectiveness of the thermal insulation system was evaluated to prevent overheating of the outer surfaces. Fig. 10 shows the temperature distribution for an operating scenario at 400 °C. A stable thermal profile was observed in the central treatment zone, with a maximum of 400.14 °C and a minimum of 399.78 °C, indicating high efficiency of the heating and insulation system under nominal conditions.

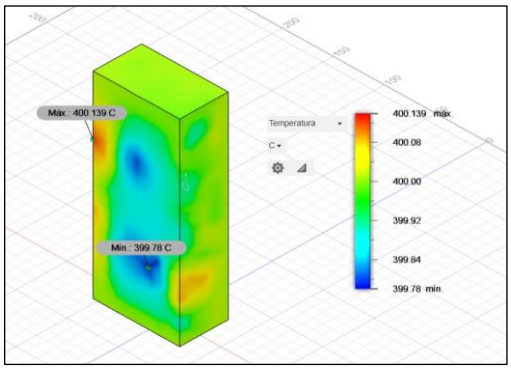

Fig. 10. Simulated temperature distribution at 400 °C. The chamber maintains the target temperature in the core, while external surfaces remain below 60 °C

As part of a thermal sensitivity analysis, the system's behavior was evaluated under more demanding scenarios by increasing the nominal temperature to 700, 900, and 1100 °C. These simulations allowed the estimation of insulation robustness in the event of control failures or extreme operating conditions. At 700 °C, as shown in Fig. 11, the internal chamber reached a maximum of 700.24 °C and a minimum of 699.62 °C without significant heat transfer to the enclosure.

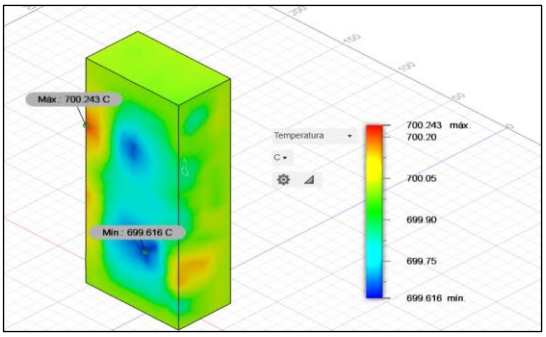

Fig. 11. Thermal profile at 700 °C. The thermal gradient intensifies, but external surfaces remain within safe limits

Fig. 12 presents the thermal behavior at 900 °C. Despite the increased thermal load, external temperatures remained within safety thresholds due to the performance of the refractory lining.

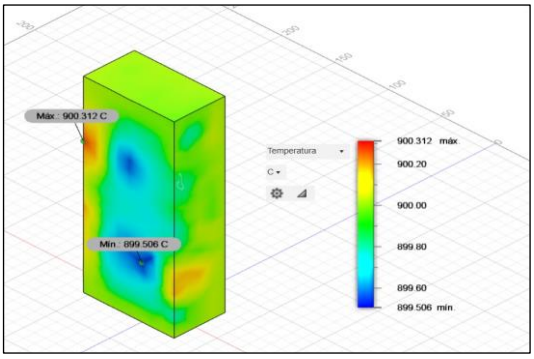

Fig. 12. Temperature distribution at 900 °C. Heat remains concentrated in the internal zone with minimal loss to the surroundings

Fig. 13 illustrates the results for the 1100 °C scenario, the highest simulated thermal load. Maximum and minimum internal temperatures were 1100.38 °C and 1099.39 °C, respectively, confirming effective thermal confinement across the treatment volume.

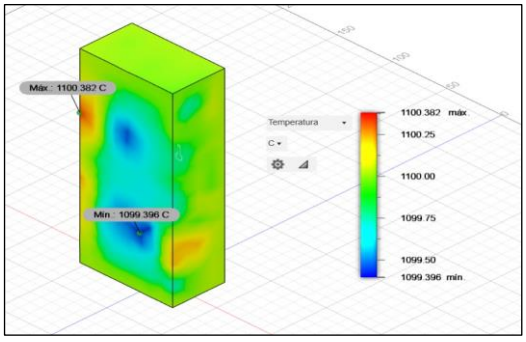

Fig. 13. Thermal map at 1100 °C. The system remains thermally contained, without critical hotspots on the outer shell

Finally, Fig. 14 compares the thermal profiles of all simulated scenarios (400, 700, 900, and 1100 °C) in an integrated view of the equipment. The comparison reveals inactive regions remained well insulated even under extreme

thermal loads, with external temperatures consistently below 60 °C.

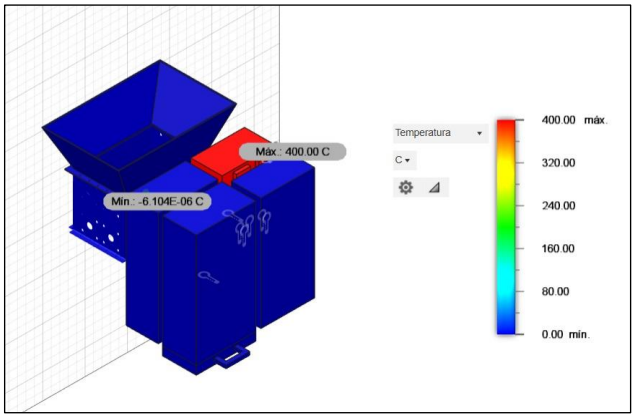

Fig. 14. Comparative thermal profiles and critical zones at different simulated temperatures

These simulations were conducted under ideal conditions, assuming no insulation degradation, residue accumulation, or power supply fluctuations. Therefore, the results should be interpreted as a preliminary numerical approximation, pending experimental validation in future project phases.

C. Volume Reduction and Impact on Final Design

The integrated system comprising double shredding, thermal evaporation, and hydraulic compaction significantly reduced the volume of hazardous medical waste. Based on technical references and the system's operating principles, the volume reduction was estimated to range between 70% and 75%, depending on waste type, moisture content, and thermal exposure time. This efficiency could be further improved by adjusting the evaporation parameters and compaction pressure. Fig. 15 shows an external view of the conceptual prototype. The main enclosure is visible, including a top-loading lid and a rear exhaust outlet that channels gases toward the purification module.

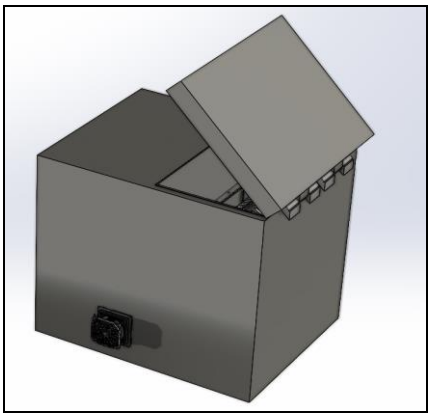

Fig. 15. External view of the compact machine, showing the arrangement of the hopper and the exhaust gas outlet

The system also incorporated a microbiological disinfection module using UV-C radiation, located at the final stage of the treatment process. Although the radiation field was not simulated, the design included UV-C lamps rated between 8 and 20 W, expected to deliver doses exceeding 100 J/m² sufficient to inactivate viruses and resistant bacteria, as reported in the scientific literature. A steam self-cleaning subsystem was integrated to ensure hygienic operation without frequent disassembly. This module performed periodic sanitation cycles targeting the feed hopper, shredding chambers, and internal ducts. Fig. 16 presents a sectional view of the whole system, highlighting the compact arrangement of the functional subsystems.

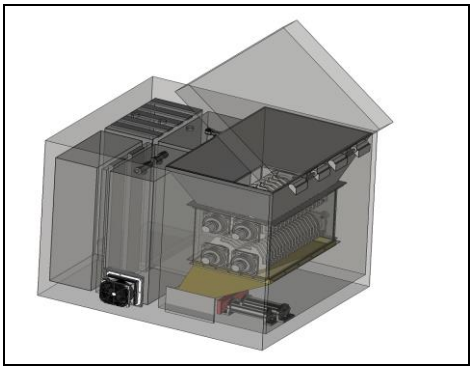

Fig. 16. Sectional view of the internal assembly, showing the shredding subsystem, evaporation chamber, compaction pistons, and UV-C module

Regarding the technical parameters derived from simulations, the selection of AISI 4340 and D2 steel for the blades was validated, with safety factors exceeding six under simulated cyclic loads. Additionally, the power ratings for the heating elements (3-5 kW) and motors (1.5-2 HP) were defined based on the operational requirements for thermal and mechanical treatment, while also considering the energy limitations typical of rural environments.

V. DISCUSSION

The simulation results supported the theoretical validation of the proposed system in terms of structural robustness, thermal efficiency, and operational safety for decentralized hazardous medical waste treatment in low-resource rural settings. From a mechanical perspective, the finite element analysis identified stress concentrations in the critical zones of the shredding subsystem, with a minimum safety factor exceeding 6. This value surpasses the recommended design threshold of 2.5 and is consistent with prior studies on biomedical waste cutting mechanisms [89], [90]. The selected materials (AISI 4340, D2, and ASTM A36 steels) also demonstrated mechanical behavior appropriate for components subjected to cyclic loading in shredding and compaction systems [91].

In terms of thermal performance, the evaporation chamber achieved stable temperatures between 400 and 600 °C within 20-25 minutes of operation, with a homogeneous thermal distribution and effective heat containment by refractory insulation. The external surface temperature remained below 60 °C, enhancing operator safety. These conditions align with intermediate thermal treatment strategies proposed by Shi et al. [92], who suggest localized disinfection as an alternative to high-temperature plasma systems operating at 1500–5000 °C [93]. Although detailed fluid-chemical simulations were not performed, the emissions treatment design includes acid neutralization through sodium bicarbonate injection, activated carbon filtration, and mechanical particle retention. Similar configurations have shown purification efficiencies exceeding 95% in industrial applications. Additionally, the

integration of a UV-C disinfection module offers a final microbiological inactivation stage, supported by its proven efficacy in clinical surface sterilization [94].

Unlike emerging approaches centered on energy recovery through pyrolysis [95], [96], the proposed system focuses on on-site neutralization, eliminating the need for external transportation and reducing biohazard exposure in rural settings. This strategy is especially relevant for remote healthcare posts in Peru and is adaptable to other regions with limited healthcare infrastructure. Nonetheless, several limitations must be acknowledged. The simulations were conducted under idealized conditions, without accounting for progressive material degradation, waste accumulation, or environmental variability typically present in high-altitude rural regions (e.g., humidity, atmospheric pressure, and heterogeneous waste composition). Moreover, the performance of the UV-C and gas purification modules has yet to be empirically validated, and their effectiveness remains to be confirmed through experimental testing. Despite these limitations, the findings establish robust preliminary design criteria for the development of a functional prototype. The next research phase should include empirical validation under real operating conditions, involving emissions monitoring, microbiological assessment, variable waste loads, and maintenance protocols suited to rural environments.

VI. CONCLUSION

This study presented the design and theoretical validation of a compact machine for the safe treatment of hazardous medical waste in rural settings. The system integrates four functional stages: double shredding, thermal evaporation, gas purification, and UV-C disinfection, which are evaluated through structural (FEA) and thermal (CFD) simulations. The results indicate that the mechanical subsystem maintains safety factors above 6.0 and that the thermal insulation effectively confines external temperatures below 60 °C, even under high thermal load scenarios. The system architecture enables an estimated waste volume reduction between 70% and 75%, in accordance with values reported in the technical literature.

Among the identified limitations, it is important to note that the analyses were exclusively simulation-based, without experimental validation of the gas purification efficiency or the germicidal performance of the UV-C module. Additionally, system performance under variations in waste moisture content or composition, as well as under critical conditions such as power outages or low electrical stability common in rural areas, has not yet been assessed.

As future work, the construction of a functional prototype and its experimental validation under real operating conditions is proposed. It is recommended to include a backup system or renewable energy sources such as solar panels or batteries to ensure continuous operation during power interruptions, and to assess their impact on operational costs and maintenance requirements. This development proposes a technically replicable solution, grounded in principles of thermal, structural, and sanitary engineering, that can contribute to the decentralization of medical waste treatment in low-infrastructure contexts.

REFERENCES

[1] S. Chakraborty, R., Raut, T. M., Rofin, S., and Chakraborty, S. "A comprehensive review of applications of multi-criteria decision-making methods in healthcare waste management." *Waste Management and Research*, 2025, doi: 10.1177/0734242X251320872.

[2] Y. Cho, P. A. Withana, J. H. Rhee, S. T. Lim, J. Y. Lim, S. W. Park, and Y. S. Ok, "Achieving the sustainable waste management of medical plastic packaging using a life cycle assessment approach," *Heliyon*, vol. 10, no. 19, Oct. 2024.

[3] A. Ranjan, S. Kaushik, M. Singh, and S. Bhutani, "Biomedical waste treatment and energy generation," *Biomedical Waste Management: Bioremediation and Recycling*, vol. 1, pp. 103-114, Sept. 2024, Doi: 10.1515/9783111305288-007.

[4] H. Pande *et al*., "Segregation of biomedical waste: Methodologies and importance," in *Biomedical Waste Management: Bioremediation and Recycling*, vol. 1, pp. 65-84, Sept. 2024.

[5] R. M. Bommi, S. V. S. Rajeev, S. Sarvepalli, V. S. Teja, and U. Supriya, "Smart Healthcare Waste Segregation and Safe Disposal," *Mathematics and Computer Science*, vol. 2, pp. 205-221, June 2024.

[6] L. W. Limenh *et al*., "Management of pharmaceutical waste from hospitals and community pharmacies in Bahir Dar and Gondar cities, Ethiopia," *BMC Health Services Research*, vol. 25, no. 1, Dec. 2025, doi: 10.1186/s12913-025-12555-6.

[7] G. Santra, "Plastic Pollution and One Health Crisis: A Burning Issue in Environmental Medicine," *Journal of Association of Physicians of India*, vol. 73, no. 3, pp. 73-83, Mar. 2025, doi: 10.59556/japi.73.0840.

[8] R. F. Asto Bonifacio, "Applications of Robotic Systems and Emerging Technologies in the Collection, Classification, and Treatment of Medical Waste: A Systematic Review," *Journal of Robotics and Control (JRC)*, vol. 6, no. 2, p. 734, 2025.

[9] A. X. Trujillo-Moscoso, C. Paredes-Schmidt, and J. C. Quiroz-Flores, "Evaluation of the environmental impact of medical waste in health centers in Peru," in *Proc. 5th South American Conf. on Industrial Engineering and Operations Management (IEOM)*, May. 2024, doi: 10.46254/SA05.20240125.

[10] C. Cayo-Rojas *et al*., "Impact of a virtual educational intervention on knowledge and awareness of biomedical waste management among Peruvian dental professionals," *Scientific Reports*, vol. 13, Dec. 2023, doi: 10.1038/s41598-023-49766-2.

[11] F. Mayta-Tovalino, A. Munive-Degregori, R. Bocanegra, R. Mendoza, J. Alvitez, and A. Temoche, "Awareness, knowledge, attitude, and practices in the management of biomedical waste: A multivariate analysis of associated factors in Peruvian students," *World Journal of Dentistry*, vol. 13, 2022, doi: 10.5005/jp-journals-10015-1887.

[12] F. G. Torres and G. E. De la Torre, "Face mask waste generation and management during the COVID-19 pandemic: An overview and the Peruvian case," *Science of the Total Environment*, vol. 786, Sep. 2021, doi: 10.1016/j.scitotenv.2021.147628.

[13] J. J. Milón Guzmán, S. L. Braga, F. A. Y. Pradelle, M. E. Díaz Coa, and C. K. Infa Mamani, "Experimental Evaluation of a Mobile Charging Station Prototype for Energy Supply in Rural and Isolated Areas during Emergency Situations," *Energies*, vol. 18, no. 3, p. 465, Jan. 2025, doi: 10.3390/en18030465.

[14] J. M. Chisholm, R. Zamani, and M. Akrami, "Sustainable waste management of medical waste in African developing countries: A narrative review," *Waste Management & Research*, vol. 39, no. 9, Jul. 2021, doi: 10.1177/0734242X211029175.

[15] S. M. Lee and D. Lee, "Effective Medical Waste Management for Sustainable Green Healthcare," *International Journal of Environmental Research and Public Health*, vol. 19, no. 22, Nov. 2022, doi: 10.3390/ijerph192214820.

[16] K. Govindan, S. Nosrati-Abarghooee, M. M. Nasiri, and F. Jolai, "Green reverse logistics network design for medical waste management: A circular economy transition through case approach," *Journal of Environmental Management*, vol. 322, Nov. 2022, doi: 10.1016/j.jenvman.2022.115888.

[17] L. Andeobu, "Medical waste and its management," in *The Palgrave Handbook of Global Sustainability, R. Brinkmann, Ed. Cham: Palgrave Macmillan*, 2023, doi: 10.1007/978-3-031-01949-4_53.

[18] D. Kim, M. M. Azad, S. Khalid, and H. S. Kim, "Data-driven surrogate modeling for global sensitivity analysis and design optimization of

medical waste shredding systems," *Alexandria Engineering Journal*, vol. 82, pp. 69-81, Nov. 2023, doi: 10.1016/j.aej.2023.108112.

[19] M. M. Azad, D. Kim, S. Khalid, and H. S. Kim, "Topology optimization and fatigue life estimation of sustainable medical waste shredder blade," *Mathematics*, vol. 10, no. 11, May 2022.

[20] M. M. Azad, D. Kim, S. Khalid, and H. S. Kim, "Structural stability analysis of medical waste sterilization shredder," *International Journal of Mechanical and Production Engineering Research and Development (IJMPERD)*, vol. 11, no. 6, pp. 409-415, Dec. 2021.

[21] J. Flizikowski, W. Kruszelnicka, and M. Macko, "The development of efficient contaminated polymer materials shredding in recycling processes," *Polymers*, vol. 13, no. 5, Feb. 2021.

[22] J. H. Wong, W. M. J. Karen, S. A. Bahrin, B. L. Chua, G. J. H. Melvin, and N. J. Siambun, "Wear mechanisms and performance of PET shredder blade with various geometries and orientations," *Machines*, vol. 10, no. 9, Sep. 2022.

[23] M. Heibeck, J. Richter, A. Hornig, T. Mütze, M. Rudolph, M. Reuter, N. Modler, and A. Filippatos, "Simulating the shredding process of multi-material structures for recyclability assessment," *Materials & Design*, vol. 232, August. 2023, doi: 10.1016/j.matdes.2023.112167.

[24] J. H. Wong, W. M. J. Karen, S. A. Bahrin, B. L. Chua, G. J. H. Melvin, and N. J. Siambun, "Wear mechanisms and performance of PET shredder blade with various geometries and orientations," *Machines*, vol. 10, no. 9, p. 760, Sep. 2022.

[25] S. Pylypaka *et al*., "Design of a Helical Shredding Drum Blade and Determination of Its Unfolding," in *Grabchenko's International Conference on Advanced Manufacturing Processes*, pp. 587-595, 2024.

[26] M. M. Azad, D. Kim, S. Khalid, and H. S. Kim, "Topology optimization and fatigue life estimation of sustainable medical waste shredder blade," *Mathematics*, vol. 10, no. 11, p. 1863, May. 2022.

[27] Z. Qiu, Y. Liu, Z. Yang, X. Ma, and X. Yang, "Analysis of blockage and wrapping by leaves in the cutting mechanism of a sugarcane leaf shredder," *Biosystems Engineering*, vol. 211, pp. 152-166, Aug. 2021.

[28] S. R. Shaik, A. K. Mahalingam, M. Palanisamy, and P. C. Kalita, "Comprehensive Review on Medical Waste Incineration," *International Journal of Global Warming*, vol. 27, no. 1, pp. 16-54, May 2022, doi: 10.1504/IJGW.2022.122793.

[29] S. Zhang *et al*., "Incineration experiment of medical waste of novel coronavirus pneumonia (COVID-19) in a mobile animal carcass incinerator," *Waste Disposal and Sustainable Energy*, vol. 3, pp. 177-183, Jun. 2021.

[30] S. E. Agustina, E. A. Pane, M. F. Nurcholis, and Arviansyah, "Design development of portable (mini) multi-function incinerator for dry medical waste handling," in *IOP Conference Series: Earth and Environmental Science*, vol. 1038, 2022.

[31] D. Wysocki and A. Szymanek, "The effectiveness of modified sodium bicarbonate in the purification of exhaust gases from HCl and HF," *Journal of Achievements in Materials and Manufacturing Engineering*, vol. 114, no. 2, Oct. 2022, doi: 10.5604/01.3001.0016.2156.

[32] J. Zheng, X. Xing, Z. Pang, S. Wang, Y. Du, and M. Lv, "Effect of Na_2CO_3, HF, and CO_2 Treatment on the Regeneration of Exhausted Activated Carbon Used in Sintering Flue Gas," *ACS Omega*, vol. 6, no. 39, Sep. 2021, doi: 10.1021/acsomega.1c03537.

[33] S. Endah Agustina, E. A. Pane, M. F. Nurcholis, and Arviansyah, "Design Development of Portable (Mini) Multi-function Incinerator for Dry Medical Waste Handling," *IOP Conf. Ser.: Earth Environ. Sci*., vol. 1038, p. 012057, 2022, doi: 10.1088/1755-1315/1038/1/012057.

[34] D. Wysocki and A. Szymanek, "The effectiveness of modified sodium bicarbonate in the purification of exhaust gases from HCl and HF," *J. Achiev. Mater. Manuf. Eng*., vol. 114, no. 2, Oct. 2022.

[35] U. O. Matthew *et al*., "Ultra Violet (UV) Light Irradiation Device for Hospital Disinfection: Control of Hospital-Acquired Infections," *International Journal of Information Communication Technologies and Human Development (IJICTHD)*, vol. 14, no. 1, pp. 1-24, 2022, doi: 10.4018/IJICTHD.313978.

[36] J. Conroy *et al*., "Robot Development and Path Planning for Indoor Ultraviolet Light Disinfection," *2021 IEEE International Conference on Robotics and Automation (ICRA)*, pp. 7795-7801, 2021.

[37] B. C. Millar and J. E. Moore, "Evaluation of a domestic steam disinfector-dryer device for disinfection of health care workers' identification lanyards," *Workplace Health & Safety*, vol. 69, no. 11, Jun. 2021. doi: 10.1177/21650799211012653.

[38] J. S. Weese, "Cleaning and disinfection," in *Greene's Infectious Diseases of the Dog and Cat*, pp. 162-170, 2021, doi: 10.1016/B978-0-323-50934-3.00014-8.

[39] U. Adak, "The sterilization and disinfection machines: sanitation and public health in the late Ottoman Empire," *Middle Eastern Studies*, vol. 58, no. 6, pp. 917-930, 2022. doi: 10.1080/00263206.2022.2027765.

[40] X. Liu, W. Liu, F. Zhou, C. Zhou, and H. Chen, "Study on the Effect of Cleaning the Da Vinci Patient Side Manipulator with a Steam Cleaner," *Sterile Supply*, vol. 3, no. 3, Oct. 2024.

[41] W. Yuzhu, X. Linyun, J. Jing, Z. Aiqi, D. Binhu, and Y. Dongdong, "Test and analysis of heat transfer in steam disinfection of matrix soil," *Journal of Chinese Agricultural Mechanization*, vol. 45, no. 6, pp. 277-283, 2024, doi: 10.13733/j.jcam.issn.2095-5553.2024.06.041.

[42] T. Liu, "Research on the stability of a hydraulic system based on nonlinear PID control," *Nonlinear Eng*., vol. 11, no. 1, pp. 494-499, 2022, doi: 10.1515/nleng-2022-0222.

[43] S. A. Al-Samarraie and I. I. Gorial, "Assessment of FLC, PID, Nonlinear PID, and SMC Controllers for Level Stabilization in Mechatronic Systems," *Journal of Robotics and Control (JRC)*, vol. 5, no. 6, pp. 1845-1861, 2024, doi: 10.18196/jrc.v5i6.23639.

[44] I. Zaitceva and B. Andrievsky, "Methods of Intelligent Control in Mechatronics and Robotic Engineering: A Survey," *Electronics*, vol. 11, no. 15, p. 2443, August. 2022.

[45] A. Safdari, A. Mansouri, M. J. Fazli, P. Zarafshan, K. Alipour, and B. Tarvirdizadeh, "PID Controller Design for a Mechatronic System using Lion Optimization Algorithm," *2025 Fifth National and the First International Conference on Applied Research in Electrical Engineering (AREE)*, pp. 1-7, 2025, doi: 10.1109/AREE63378.2025.10880235.

[46] S. Kapoulea, C. Psychalinos, A. S. Elwakil, and S. H. HosseinNia, "Realizations of fractional-order PID loop-shaping controller for mechatronic applications," *Integration*, vol. 80, pp. 5-12, Sep. 2021, doi: 10.1016/j.vlsi.2021.04.009.

[47] G. Pereira das Neves and B. Augusto Angélico, "Model-free control of mechatronic systems based on algebraic estimation, " *Asian J. Control*, 2021, doi: 10.1002/asjc.2596.

[48] T. Staessens, T. Lefebvre, and G. Crevecoeur, "Adaptive Control of a Mechatronic System Using Constrained Residual Reinforcement Learning," in *IEEE Transactions on Industrial Electronics*, vol. 69, no. 10, pp. 10447-10456, Oct. 2022, doi: 10.1109/TIE.2022.3144565.

[49] N. Malekpoor Joneghani, N. Zarrinpoor, and M. Eghtesadifard, "A mathematical model for designing a network of sustainable medical waste management under uncertainty," *Computers & Industrial Engineering*, vol. 171, Sep. 2022.

[50] A. Amirteimoori, E. B. Tirkolaee, A. Amirteimoori, A. Khakbaz, and V. Simic, "A novel parallel heuristic method to design a sustainable medical waste management system," *J. Clean. Prod*., vol. 452, May. 2024, doi: 10.1016/j.jclepro.2024.141897.

[51] M. A. Shbool *et al*., "Predictive Modeling of Chemical Waste Generation in Healthcare Facilities: Enhancing Waste Management Strategies," *Athens J. Sci*., vol. 12, pp. 1-23, 2025.

[52] E. B. Tirkolaee and N. S. Aydin, "A Sustainable Medical Waste Collection and Transportation Model for Pandemics," *Waste Manag. Res*., vol. 39, 2021, doi: 10.1177/0734242X211000437.

[53] A. E. Torkayesh, H. R. Vandchali, and E. B. Tirkolaee, "Multi-Objective Optimization for Healthcare Waste Management Network Design with a Sustainability Perspective," *Sustainability*, vol. 13, no. 15, 2021, doi: 10.3390/su13158279.

[54] M. Rahiminia *et al*., "A novel data-driven patient and medical waste queueing-inventory system under pandemic: A real-life case study," *Int. J. Prod. Res*., vol. 63, no. 2, pp. 418-434, May 2023.

[55] J. Ellinger, T. Semm, and M. F. Zaeh, "Dimensionality reduction of high-fidelity machine tool models by using global sensitivity analysis," *Journal of Manufacturing Science and Engineering*, vol. 144, no. 5, p. 051010, May 2022.

[56] S. Razavi *et al*., "The future of sensitivity analysis: an essential discipline for systems modeling and policy support," *Environmental Modelling & Software*, vol. 137, p. 104954, Jun. 2021.

[57] M. Kouhen, A. Dimitrova, G. S. Scippa, and D. Trupiano, "The Course of Mechanical Stress: Types, Perception, and Plant Response," *Biology*, vol. 12, no. 2, p. 217, Jan. 2023.

[58] A. Ali, S. S. R. Koloor, A. H. Alshehri, and A. Arockiarajan, "Carbon nanotube characteristics and enhancement effects on the mechanical properties of polymer-based materials and structures - A review," *Journal of Materials Research and Technology*, vol. 24, pp. 6495-6521, May-June. 2023, doi: 10.1016/j.jmrt.2023.04.072.

[59] Y. Zhang *et al*., "State of the art of finite element analysis in mechanical clinching," *International Journal of Precision Engineering and Manufacturing - Green Technology*, vol. 9, no. 4, pp. 1191-1214, 2022.

[60] A. McCulloch *et al*., "Large-scale finite element analysis of the beating heart," in *High-Performance Computing in Biomedical Research*, pp. 27-49, 2020.

[61] T. C. N. Nguyen *et al*., "Static bending analysis of variable thickness microplates using the finite element method and modified couple stress theory," *Journal of Science and Technique*, vol. 17, no. 3, pp. 13-26, 2022.

[62] Y. Cao *et al*., "A new efficient finite element analysis method for powder bed fusion additive manufacturing," *Additive Manufacturing*, vol. 46, p. 102187, 2021.

[63] G. Zhen *et al*., "Mechanical stress determines the configuration of TGFβ activation in articular cartilage," *Nature Communications*, vol. 12, p. 1706, Mar. 2021.

[64] M. Jażdżewska, M. Bartmański, A. Zieliński, and D. B. Kwidzińska, "Effect of Laser Treatment on Intrinsic Mechanical Stresses in Titanium and Some of Its Alloys," *Applied Sciences*, vol. 13, no. 10, p. 6276, May. 2023, doi: 10.3390/app13106276.

[65] B. Su, S. Liu, P. Zhang, J. Wu, and Y. Wang, "Mechanical properties and failure mechanism of overlap structure for cord-rubber composite," *Composite Structures*, vol. 274, p. 114350, Oct. 2021.

[66] E. Menacho-Mendoza, R. Cedamanos-Cuenca, and A. Díaz-Suyo, "Stress analysis and factor of safety in three dental implant systems by finite element analysis," *The Saudi Dental Journal*, vol. 34, no. 7, pp. 579-584, Nov. 2022, doi: 10.1016/j.sdentj.2022.08.006.

[67] N. F. Al Zoubi, F. Tarlochan, and H. Mehmood, "Mechanical and Fatigue Behavior of Cellular Structure Ti-6Al-4V Alloy Femoral Stems: A Finite Element Analysis," *Applied Sciences*, vol. 12, no. 9, p. 4197, Apr. 2022, doi: 10.3390/app12094197.

[68] A. B. Prasetiyo and K. A. Sekarjati, "Finite Element Simulation of Power Weeder Machine Frame," *Indonesian Journal of Computing, Engineering, and Design (IJoCED)*, vol. 4, no. 2, pp. 25-34, Oct. 2022.

[69] A. I. Mohammed *et al*., "An application of FEA and machine learning for the prediction and optimisation of casing buckling and deformation responses in shale gas wells in an in-situ operation," *Journal of Natural Gas Science and Engineering*, vol. 95, Nov. 2021.

[70] P. H. Tjahjanti, A. Fahruddin, A. Hermawanto, and S. Firmansyah, "Effective and Efficient Design and Manufacture of a Plastic Waste Press Machine," *Jurnal Terapan Teknik Mesin (JTTM)*, vol. 4, no. 2, 2023, doi: 10.37337/jttm.v4i2.627.

[71] E. Esim and E. Benzer, "Structural Analysis of an Industrial Foam Crusher Machine Using the Finite Element Method," *Avrupa Bilim ve Teknoloji Dergisi*, pp. 343-350, Dec. 2021.

[72] J. Rishmany and R. Imad, "Finite Element and Multibody Dynamics Analysis of a Ball Mill Glass Crusher," *Modelling and Simulation in Engineering*, Mar. 2023, doi: 10.1155/2023/1905702.

[73] M. Egbo, "A Review of the Thermal Performance of Vapor Chambers and Heat Sinks: Critical Heat Flux, Thermal Resistances, and Surface Temperatures," *International Journal of Heat and Mass Transfer*, vol. 183, Feb. 2022.

[74] D. Xie, Y. Sun, G. Wang, S. Chen, and G. Ding, "Significant factors affecting heat transfer performance of vapor chamber and strategies to promote it: A critical review," *International Journal of Heat and Mass Transfer*, vol. 175, 121132, Aug. 2021.

[75] X. Ye, X. An, H. Zhang, S. Wang, B. Guo, and A. Yu, "Process simulation on atomization and evaporation of desulfurization wastewater and its application," *Powder Technology*, vol. 389, pp. 178-188, Sep. 2021, doi: 10.1016/j.powtec.2021.05.024.

[76] C. Liu, D. Hu, Q. Li, X. Chen, Z. Zhang, and F. Zhou, "Vapor chamber with two-layer liquid supply evaporator wick for high-heat-flux devices," *Applied Thermal Engineering*, vol. 190, p. 116803, May 2021.

[77] H. M. Maghrabie, A. G. Olabi, A. H. Alami, M. A. Radi, F. Zwayyed, T. Salamah, T. Wilberforce, and M. A. Abdelkareem, "Numerical simulation of heat pipes in different applications," *International Journal of Thermofluids*, vol. 16, p. 100199, Nov. 2022.

[78] Y. Feng *et al*., "The effects of process parameters on the mechanical properties and degradation behavior of Fe/HA biodegradable materials", *J. Biomaterials Appl*., Dec. 2024.

[79] E. Kornfellner *et al*., "Measured and simulated mechanical properties of additively manufactured matrix-inclusion multimaterials fabricated by material jetting", *3D Print. Med*., vol. 10, no. 1, Feb. 2024.

[80] M. M. Alnsour, R. A. Alamoush, N. Silikas, and J. D. Satterthwaite, "The effect of erosive media on the mechanical properties of CAD/CAM composite materials", *J. Functional Biomaterials*, vol. 15, no. 10, p. 292, Oct. 2024, doi:10.3390/jfb15100292.

[81] J. P. Whiteley, C. P. Brown, and E. A. Gaffney, "Sensitivity of cartilage mechanical behaviour to spatial variations in material properties", *J. Mech. Behav. Biomed. Mater*., p. 106575, May. 2024.

[82] E. Dincel, "Advanced mechanical ventilation modes: Design and computer simulations", *Comput. Methods Biomechanics Biomed. Eng*., pp. 1–14, Nov. 2020.

[83] L. G. Sun *et al*., "Nanostructural metallic materials: Structures and mechanical properties," *Materials Today*, vol. 38, pp. 114–135, 2020.

[84] Y. Zhu and X. Wu, "Heterostructured materials," *Progress in Materials Science*, vol. 131, p. 101019, 2023.

[85] Y. A. Shah *et al*., "Mechanical properties of protein-based food packaging materials," *Polymers*, vol. 15, no. 7, p. 1724, 2023.

[86] T. Liu *et al*., "Characterization and thermal modeling of a miniature silicon vapor chamber for die-level heat redistribution," *International Journal of Heat and Mass Transfer*, vol. 152, p. 119569, 2020.

[87] M. Benedetti *et al*., "Architected cellular materials: A review on their mechanical properties towards fatigue-tolerant design and fabrication," *Materials Science and Engineering: R: Reports*, vol. 144, p. 2021.

[88] T. Ren *et al*., "Elucidating mesostructural effects on thermal conductivity for enhanced insulation applications," *Small*, 2025.

[89] F. Huang *et al*., "Numerical study and multi-objective optimization of medical waste shredding tools: A DEM-FEM coupling approach," *Adv. Powder Technol*., vol. 35, no. 6, p. 104491, Jun. 2024.

[90] D. Kim, M. M. Azad, S. Khalid, and H. S. Kim, "Sensitivity Analysis of Medical Waste Sterilization Shredder Using Surrogate Model," *Trans. Korean Soc. Mech. Eng*, vol. 47, no. 1, pp. 71-77, Jan. 2023.

[91] A. H. Raheem, H. K. Kadhom, and A. A. Hussein, "Finite Element Analysis of Smart Waste Container," *AIP Conf. Proc*., vol. 3002, 2024, doi: 10.1063/5.0209557.

[92] H. Shi, P. Wang, and S. Wang, "Analysis of the Impact of Plasma Jet Mode on Medical Waste Gasification Furnace," in *IEEE Transactions on Plasma Science*, vol. 52, no. 6, pp. 2157-2167, June 2024.

[93] A. R. Galaly, "Sustainable Development Solutions for the Medical Waste Problem Using Thermal Plasmas," *Sustainability*, vol. 14, no. 17, p. 11045, Sep. 2022, doi: 10.3390/su141711045.

[94] A. Mohtasebi, R. A. Sarvestani, H. Dabiri, M. Sadani, N. Alavi, and M. Abtahi, "Effective methods for decontaminating healthcare waste: Ozone and UV-C radiation process," *Journal of the Air & Waste Management Association*, vol. 74, no. 10, pp. 743-752, Sep. 2024.

[95] G. Su, H. C. Ong, S. Ibrahim, I. M. R. Fattah, M. Mofijur, and C. T. Chong, "Valorisation of medical waste through pyrolysis for a cleaner environment: Progress and challenges," *Environmental Pollution*, vol. 279, p. 116934, Jun. 2021.

[96] J. Y. Kim, J. Park, D.-J. Lee, Y.-B. Choi, and E. E. Kwon, "Sustainable management of medical plastic waste through carbon dioxide-assisted pyrolysis," *Chemosphere*, vol. 364, 143266, Sep. 2024, doi: 10.1016/j.chemosphere.2024.143266.